

Core and surface microgel mechanics are differentially sensitive to alternative crosslinking concentrations

Himansu Mohapatra¹, Terra M. Kruger¹, Thiranjeeva I. Lansakara², Alexei V. Tivanski² and Lewis L. Stevens^{1*}

1. Division of Pharmaceutics and Translational Therapeutics, College of Pharmacy, The University of Iowa, Iowa City, IA 52242

2. Department of Chemistry, The University of Iowa, Iowa City, IA 52242

Supporting Information

AFM nanoindentation analysis of pS-co-NIPAM, pS and pNIPAM particles.

AFM nanoindentation¹⁻² technique was utilized to obtain Young's modulus (stiffness) values of individual pS-co-NIPAM, pS and pNIPAM particles. The Young's modulus was determined by fitting the loading force *versus* indentation depth approach data to Jonsen-Kendall-Roberts (JKR) model³.

$$a_{JKR} = \frac{3R^* F_{JKR}}{4E^*} \quad (1)$$

$$F_{JKR} = F + 3\pi WR^* + \sqrt{6\pi WR^* + 9\pi^2 W^2 R^{*2}} \quad (2)$$

$$h_{JKR} = \frac{a_{JKR}^2}{R^*} - \sqrt{\frac{2\pi W a_{JKR}}{E^*}} \quad (3)$$

Where a_{JKR} , F_{JKR} and h_{JKR} are the contact area radius, force acting between two spheres and indentation depth, respectively. W is the work of adhesion which can be determined directly by measuring the adhesion force between AFM tip and pS-co-NIPAM particles using the retract force *versus* vertical piezo position data⁴.

$$\frac{1}{R^*} = \frac{1}{R_1} + \frac{1}{R_2} \quad (4)$$

$$\frac{1}{E^*} = \frac{1 - \nu_1^2}{E_1} + \frac{1 - \nu_2^2}{E_2} \quad (5)$$

Where R^* and E^* are the effective radius and effective Young's modulus of AFM tip and pS-co-NIPAM spheres. R_1 , ν_1 , E_1 and R_2 , ν_2 , E_2 are the radius, Poisson's ratio and Young's modulus for tip and pS-co-NIPAM particle respectively.

JKR model was preferred over Hertzian contact model due to the observation of adhesive forces between AFM tip and pS-co-NIPAM particles which were typically of ca 2 nN - 4 nN. AFM nanoindentation experiments were performed using 8 different Si_3N_4 tips having a spring constant range of 0.2 – 0.8 N/m. Reported height values of nanoparticles were an average of ~100 single

particles which were obtained from AFM height images. For the Young's modulus calculations, tip radius of curvature of 10 nm and the Poisson's ratio of Si_3N_4 AFM tip of 0.25 were used. Poisson's ratios which were calculated with reduced BLS frequencies as mentioned in text were used for pS-co-NIPAM samples when data were fit to the JKR model. Based on the statistical analysis, force plots which yielded extremely high stiffness values and low stiffness values were a result of tip contacting the hard Si wafer surface and the edges of pS-co-NIPAM particles, therefore those force curves were excluded from force curve analysis.⁵ Typically, as a result of such analysis, ca 10% of the total force plots were excluded. Average Young's modulus values reported in this study for each particle composition are based from averaging of ~60 force *versus* indentation curves.

Nanoindentation on pS was done using a 25 nm tip radius of curvature having Pt coated tip (Nanosensors, Switzerland). This was because force curves and AFM images showed plastic deformation on pS nano-spheres when the Si_3N_4 tips with 10 nm tip radius of curvature were used. The spring constant of this Pt tip was 2.55 N/m as determined from the thermal noise method⁶. Similar to the above, data were fit to the JKR model.

Figure S1. AFM height images of pS-co-NIPAM, pS and, pNIPAM particles

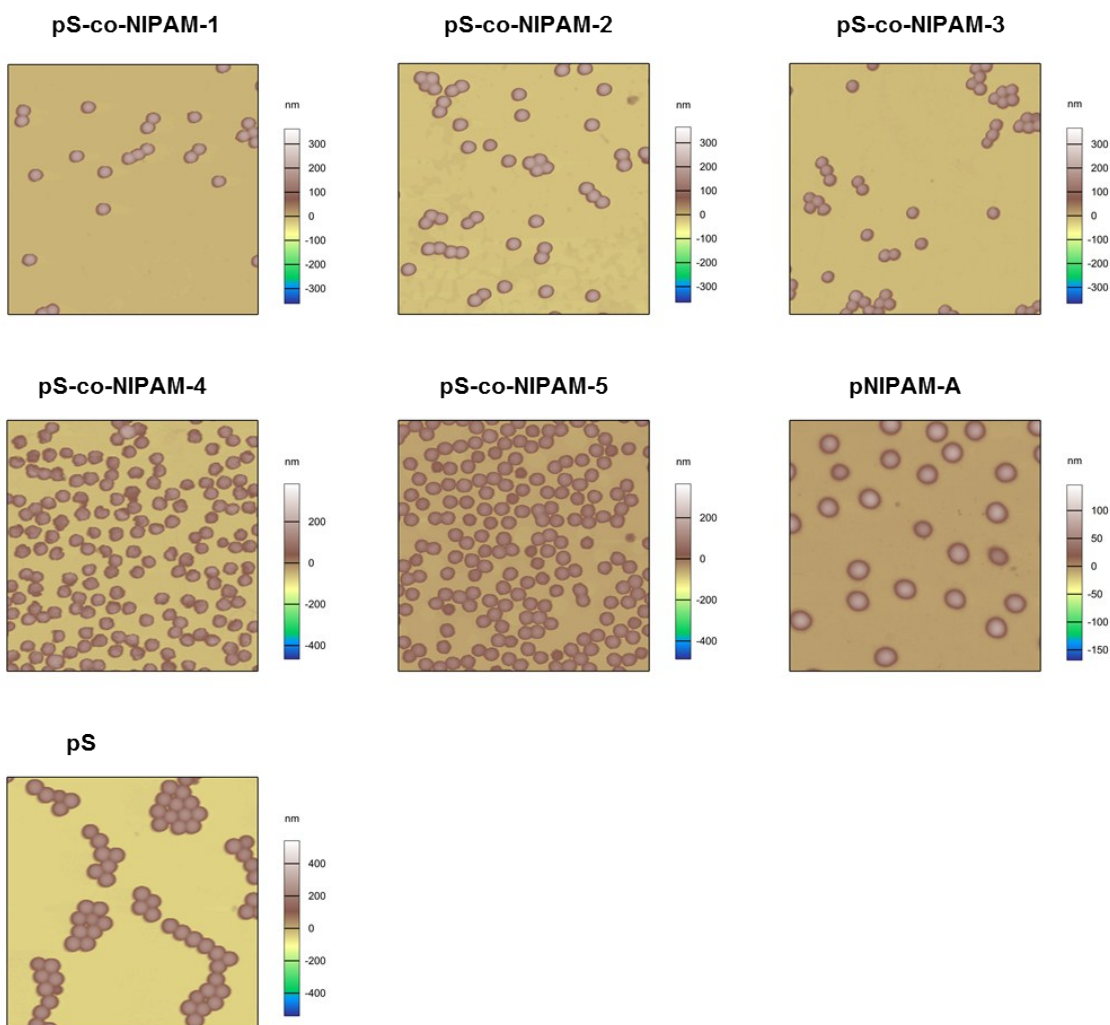


Figure S2. Representative force-displacement curves for pS, the pS-co-NIPAM series and pNIPAM-B.

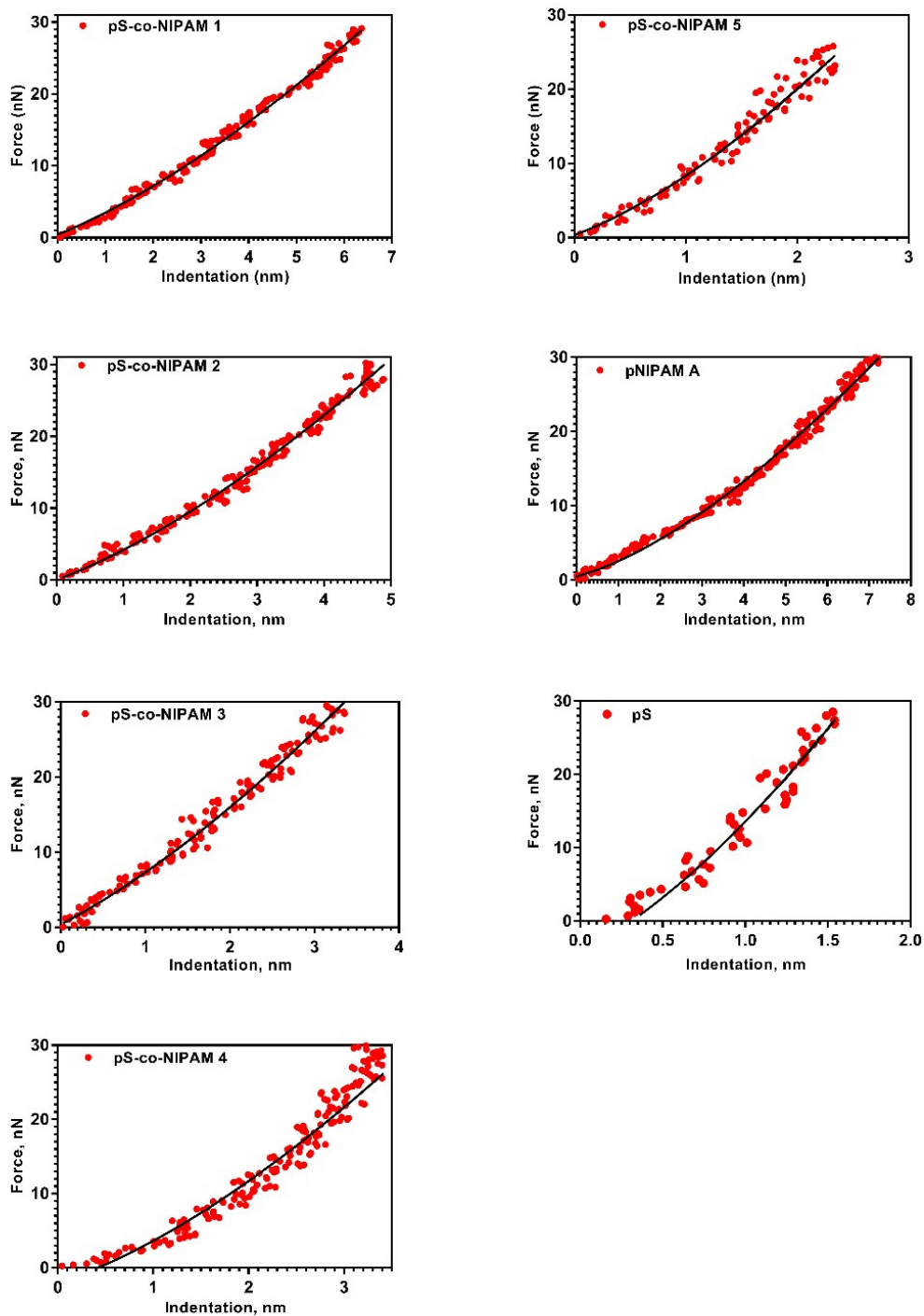


Figure S3. Illustrative example of the insensitivity of the predicted particle frequency calculation to V_L . For this example, $D = 170$ nm and $V_T = 1100$ m/s. The specific spheroidal mode (n,l) is shown in the legend.

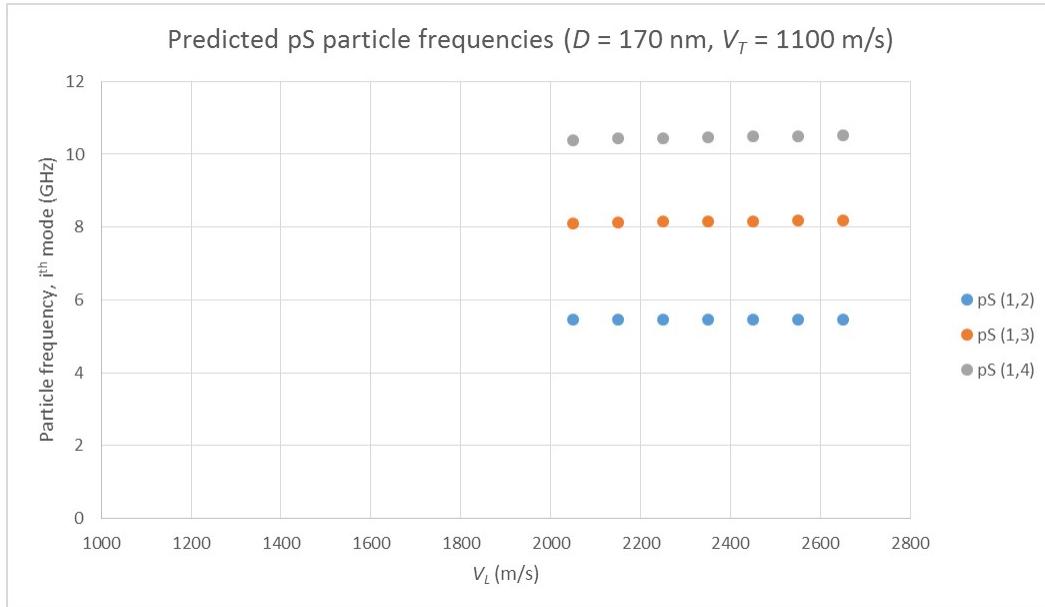
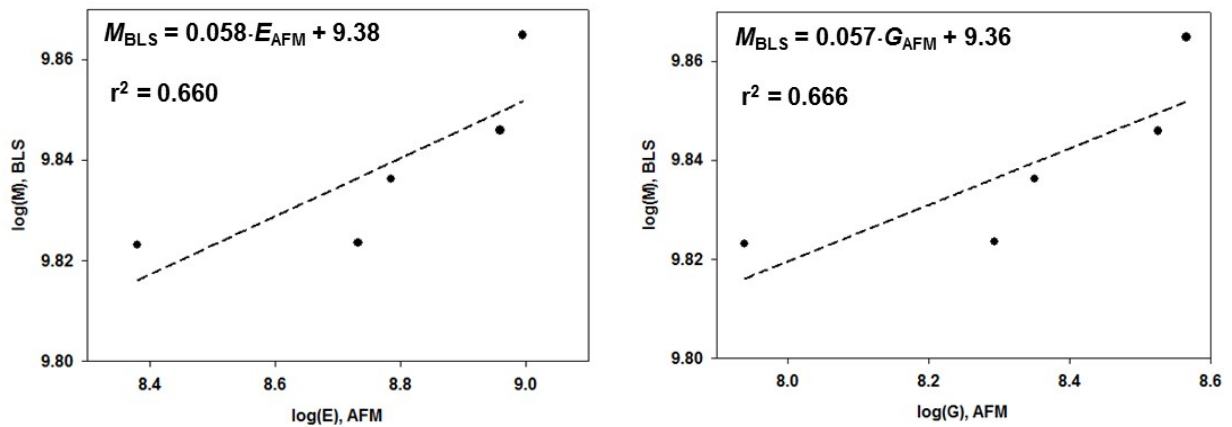


Figure S4. Log-log transformation of mechanical moduli provided from AFM nanoindentation and BLS.



References

1. Chung, P. C.; Glynos, E.; Green, P. F., The Elastic Mechanical Response of Supported Thin Polymer Films. *Langmuir* **2014**, *30* (50), 15200-15205.
2. Tan, S.; Sherman, R. L.; Ford, W. T., Nanoscale Compression of Polymer Microspheres by Atomic Force Microscopy. *Langmuir* **2004**, *20* (17), 7015-7020.
3. Johnson, K. L.; Kendall, K.; Roberts, A. D., Surface Energy and the Contact of Elastic Solids. *Proceedings of the Royal Society of London. A. Mathematical and Physical Sciences* **1971**, *324* (1558), 301-313.
4. Rupasinghe, T. P.; Hutchins, K. M.; Bandaranayake, B. S.; Ghorai, S.; Karunatilake, C.; Bučar, D. K.; Swenson, D. C.; Arnold, M. A.; Macgillivray, L. R.; Tivanski, A. V., Mechanical Properties of a Series of Macro- and Nanodimensional Organic Cocrystals Correlate with Atomic Polarizability. *Journal of the American Chemical Society* **2015**, *137* (40), 12768-12771.
5. Guo, D.; Li, J.; Xie, G.; Wang, Y.; Luo, J., Elastic Properties of Polystyrene Nanospheres Evaluated with Atomic Force Microscopy: Size Effect and Error Analysis. *Langmuir* **2014**, *30* (24), 7206-7212.
6. Hutter, J. L.; Bechhoefer, J., Calibration of atomic-force microscope tips. *Review of Scientific Instruments* **1993**, *64* (7), 1868-1873.